

# DEUTSCHES ELEKTRONEN-SYNCHROTRON DESY

DESY 87-166  
SLAC-PUB-4506  
December 1987



## SEARCH FOR TAU DECAYS TO THE ETA MESON

by

T. Skwarnicki

*Deutsches Elektronen-Synchrotron DESY, Hamburg*

ISSN 0418-9833

NOTKESTRASSE 85 · 2 HAMBURG 52

DESY behält sich alle Rechte für den Fall der Schutzrechtserteilung und für die wirtschaftliche Verwertung der in diesem Bericht enthaltenen Informationen vor.

DESY reserves all rights for commercial use of information included in this report, especially in case of filing application for or grant of patents.

To be sure that your preprints are promptly included in the  
HIGH ENERGY PHYSICS INDEX ,  
send them to the following address ( if possible by air mail ) :

DESY  
Bibliothek  
Notkestrasse 85  
2 Hamburg 52  
Germany

# SEARCH FOR TAU DECAYS TO THE ETA MESON

Tomasz Skwarnicki

*Deutsches Elektronen-Synchrotron DESY  
Notkestr. 85, 2000 Hamburg 52, Germany*

(Representing The Crystal Ball Collaboration [1])

## Abstract

Using a large sample of 530 000  $\tau$  leptons collected by the Crystal Ball experiment at the  $e^+e^-$  storage ring DORIS-II, we have searched for  $\tau$  decays to the  $\eta$  meson. No  $\eta$  signal is found in the inclusive analysis,  $\tau \rightarrow \eta X$ , of 1-prong decays, leading to the upper limits,  $\text{BR}(\tau^- \rightarrow \nu \pi^- \eta) < 0.3\%$ ,  $\text{BR}(\tau^- \rightarrow \nu \pi^- \pi^0 \eta) < 0.9\%$ ,  $\text{BR}(\tau^- \rightarrow \nu \pi^- \pi^0 \pi^0 \eta) < 3.1\%$ ,  $\text{BR}(\tau^- \rightarrow \nu \pi^- \eta \eta) < 2.5\%$  (95% CL). The decays,  $\tau^- \rightarrow \nu \pi^- \eta$  and  $\tau^- \rightarrow \nu \pi^- \pi^0 \eta$ , are also not found in the exclusive analyses, while  $\text{BR}(\tau^- \rightarrow \nu \pi^- \pi^0) = (22.7 \pm 0.9 \pm 3.0)\%$  and  $\text{BR}(\tau^- \rightarrow \nu \pi^- \pi^0 \pi^0) = (7.0 \pm 0.7 \pm 1.4)\%$  are measured in accord with the expectations. The hadronic final state,  $\pi^- \pi^0 \pi^0$ , is reconstructed in  $\tau$  decays for the first time. The results are preliminary.

*Analysis presented at  
the International Europhysics Conference  
on High Energy Physics,  
Uppsala, Sweden, June 25-July 1, 1987.*

## 1 Introduction

Decays of the  $\tau$  lepton have been well understood both experimentally [2] and theoretically, [3] except for channels with a charged particle and neutral mesons. It is notable that the inclusive measurements of the 1-prong branching ratio [4] ( $86.6 \pm 0.3\%$ ) are higher than the sum of all branching ratios measured or predicted for the exclusive channels belonging to this topology ( $< 80\%$  at 90% CL). Some measurements [5,6] attribute this excess to the channels involving neutral mesons. Because  $\tau$  lepton decays to the  $\eta$  meson would contribute to the 1-prong topology 70% of the time, [7] the existence of such decays at the few percent level could account for the missing 1-prong branching ratio. This is, however, not expected theoretically [8]. Nevertheless, the HRS collaboration recently claimed an observation of second class current decays,  $\tau^- \rightarrow \nu \pi^- \eta$ , with a branching ratio of  $(5.1 \pm 1.5)\%$  [9]. There was also evidence for an inclusive  $\eta$  signal,  $\tau \rightarrow \eta X$ , in the preliminary analysis of the Crystal Ball data presented last year [10].

Presented here, is a final analysis of that Crystal Ball data. The  $\eta$  signal found previously is shown to come from the non- $\tau$  background. A new inclusive analysis sets upper limits on the  $\eta$  production in  $\tau$  decays. Our measurement gives the most stringent limits on the decays<sup>1</sup>,  $\tau^- \rightarrow \nu \pi^- \eta$  and  $\tau^- \rightarrow \nu \pi^- \pi^0 \eta$ . The inclusive analysis is cross-checked by exclusive analyses of the final states with one or two neutral mesons. Again, there is no evidence for  $\tau^- \rightarrow \nu \pi^- \eta$  and  $\tau^- \rightarrow \nu \pi^- \pi^0 \eta$  decays, whereas the decays,  $\tau^- \rightarrow \nu \pi^- \pi^0$  and  $\tau^- \rightarrow \nu \pi^- \pi^0 \pi^0$ , are observed at the expected [3] rates. Since the decays,  $\tau^- \rightarrow \nu \pi^- \pi^0 \pi^0$ , are reconstructed for the first time, we describe this analysis at some length.

The Crystal Ball detector, with good photon detection and a large sample of  $\tau$  decays, is an appropriate tool for studies of  $\tau$  decays to final states with  $\pi^0$ s and  $\eta$ s which very often decay to  $\gamma\gamma$ . The Crystal Ball detector consists of a spherical shell of NaI(Tl) crystals, which provides good energy resolution for electromagnetically showering particles,  $\Delta E/E = 2.7\%/\sqrt{E}$ , over a large solid angle, 85% of  $4\pi$ . Charged particles are detected in a system of proportional tube chambers, with charge division readout installed inside the electromagnetic calorimeter. Momenta of charged particles are not measured as there is no magnetic field in the detector. A further description of the Crystal Ball detector has been published in detail elsewhere [11].

The data were collected at the DORIS-II storage ring at DESY in  $e^+e^-$  center-of-mass energy range from 9.4 GeV to 10.6 GeV. The data sample used corresponds to an integrated luminosity of  $256 \text{ pb}^{-1}$  and  $(534 \pm 22) \cdot 10^3$   $\tau$  leptons produced. The luminosity is measured using large angle Bhabha scattering events with accuracy of better than 3%. The number of  $\tau$  leptons is obtained using the radiatively corrected QED cross section for  $e^+e^- \rightarrow \tau^+\tau^-$  and the measured luminosity [12]. Additional contributions to the  $\tau$  sample come from the  $\Upsilon(1S)$  and  $\Upsilon(2S)$  resonance decays. It is calculated from the measured numbers of the resonances produced in our data and their leptonic branching ratios,  $B_{\mu\mu}$ .

## 2 Data Selection

Events  $e^+e^- \rightarrow \tau^+\tau^-$  are selected in a 1-1-prong topology. The first  $\tau$  lepton decays to a charged prong and photons, whereas the second  $\tau$  decays to an isolated charged prong which is *not* accompanied by any photons. The latter, called the "tagging prong," gets its main

<sup>1</sup> In this paper,  $\tau^-$  is used symbolically for the both charged states.

contributions from the well known decay modes,  $\tau^- \rightarrow \nu e^- \bar{\nu}_e$ ,  $\tau^- \rightarrow \nu \mu^- \bar{\nu}_\mu$  and  $\tau^- \rightarrow \nu \pi^-$ , which add up to almost half of all  $\tau$  decays. The most important event selection criteria are listed below:

- Two charged tracks are found in the wire chambers with an opening angle of at least  $90^\circ$ .
- At most, ten separated energy clusters are detected in the calorimeter (selects low multiplicity events).
- A cut on the second Fox-Wolfram moment is made, [13]  $H_2 > 0.45$  to select a jet-jet topology.
- Large energy flow transverse to the beam directions is required [14],  $E_T > 1.5$  GeV to suppress beam-gas and two-photon events.
- No energy cluster above 85% of the beam energy is allowed, which suppresses radiative Bhabha events.
- The total momentum vector of the neutral energy is calculated. The charged track closer to the neutral momentum vector is considered a charged- $\pi$  candidate associated with production of neutral mesons. The pseudo invariant mass of the charged- $\pi$  candidate and of the neutral system may not be larger than the  $\tau$  mass. This mass is obtained from calorimeter measurements.

At this point, the data selection splits into the inclusive and exclusive analyses which will be described separately.

### 3 Inclusive Analysis of $\tau \rightarrow \eta X$

A neutral energy cluster with a transverse energy spread in the calorimeter consistent with a single electromagnetic shower is classified as a photon. In the inclusive analysis, all photons with an energy above 50 MeV are combined into pairs in the search for an  $\eta \rightarrow \gamma\gamma$  signal. Photons from the reconstructed  $\pi^0$  decays are not used in the  $\eta$  search. The distribution of the invariant mass of  $\gamma\gamma$ -pairs,  $M_{\gamma\gamma}$ , from the selected events is plotted in Fig. 1. There is no peak observed at the  $\eta$  mass. A shape of the expected  $\eta$  signal is obtained from the Monte Carlo simulation of various  $\tau$  decays to  $\eta$ . It is represented by a Gaussian, with a width of 26 MeV, modified by a power-law tail on the low-mass side. A fit of the  $\eta$  peak on a smooth polynomial background gives  $(-10 \pm 23)$   $\eta$  counts. A detection efficiency strongly depends upon a photon multiplicity in the  $\tau$  decay, decreasing rapidly due to the increased overlap probability. This is demonstrated in Fig. 1 by plotting sizes of the expected signals for the different  $\tau \rightarrow \eta$  channels, assuming a branching ratio of 5%. Thus, we present an upper limit for each channel independently,

$$\begin{aligned} \text{BR}(\tau^- \rightarrow \nu \pi^- \eta) &< 0.3\% \text{ (95\% CL)}, \\ \text{BR}(\tau^- \rightarrow \nu \pi^- \pi^0 \eta) &< 0.9\% \text{ (95\% CL)}, \\ \text{BR}(\tau^- \rightarrow \nu \pi^- \pi^0 \pi^0 \eta) &< 3.1\% \text{ (95\% CL)}, \\ \text{BR}(\tau^- \rightarrow \nu \pi^- \eta \eta) &< 2.5\% \text{ (95\% CL)}. \end{aligned}$$

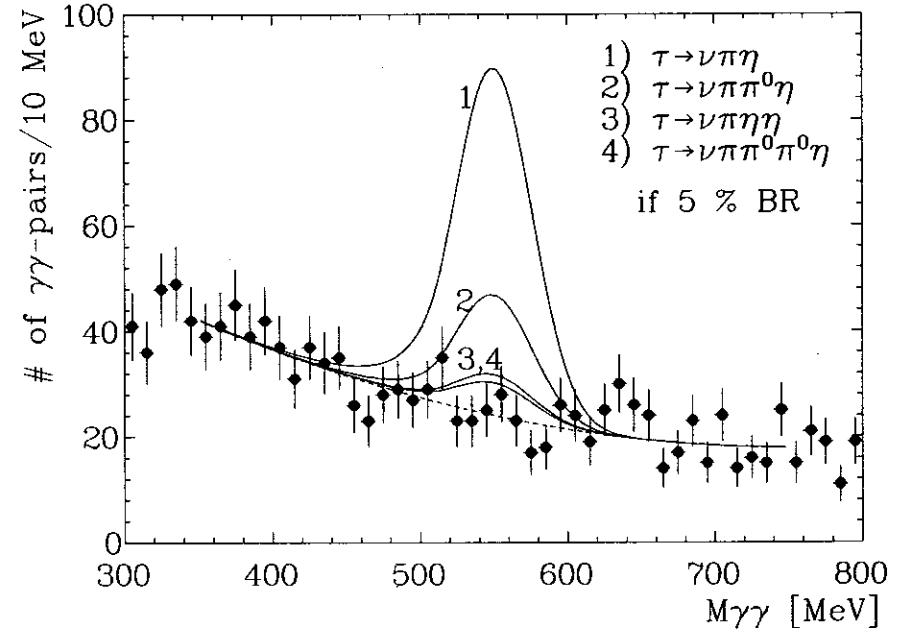


Figure 1: Inclusive distribution of two-photon invariant masses in 1-prong  $\tau$  decays. Sizes of the expected  $\eta$  signals for 5% branching ratio of various  $\tau$  decay modes are shown by the solid curves.

In the efficiency calculation, the above decays have been simulated by phase space models. A systematic uncertainty of 20% in the branching ratio calculations is folded into the upper limits. The systematic error includes uncertainties in the number of  $\tau$  leptons produced and in the efficiency calculation. It is dominated by fluctuations of the Monte Carlo data.

Our event sample in the inclusive analysis contains unknown contamination of the non- $\tau$  background. A subtraction of the background would only improve the upper limits, therefore, it is not necessary.

The first report on the status of our inclusive analysis was communicated to the Berkeley Conference, 1986 [10]. A significant  $\eta$  peak was observed in the inclusive  $M_{\gamma\gamma}$  distribution in the event sample biased towards  $\tau^+\tau^-$  pairs. Selection criteria were, however, different than described here. The topological constraints were looser, (no multiplicity cut, no cut on the angle between the charged particles, no cut on H2, etc). Instead, a loose electron identification cut was applied on one of the two charged tracks. The electron cut was designed to tag  $\tau^+\tau^-$  events on  $\tau^- \rightarrow \nu e^- \bar{\nu}_e$  decays, but still accepting some contribution from charged pions in  $\tau^- \rightarrow \nu \pi^-$  and  $\tau^- \rightarrow \nu \rho^-$  decays. Luminosity was half of that used in the analysis described here.

Background studies, based on the Monte Carlo simulations of  $\gamma\gamma$ -processes and  $e^+e^-$  annihilation to hadrons, show that our sample was predominantly due to  $\tau^+\tau^-$  decays. Some distributions, such as energy distributions of "electrons," agreed with the Monte Carlo simulation of  $\tau^+\tau^-$  events. Therefore, the signal was presented as preliminary evidence for  $\tau$  decays to  $\eta$ . However, due to the incomplete background studies (see [10]), the branching ratio was not calculated and an analysis was not published while awaiting more detailed checks. In fact, further investigations have shown serious inconsistencies between behavior of the  $\eta$  signal and the Monte Carlo simulations of various  $\tau$  decays to  $\eta$ . Examples are given below. The distribution of the cosine of the angle between the two charged prongs,  $\cos(\text{charged, charged})$ , is plotted in Fig. 2(a). A characteristic peak for  $\tau^+\tau^-$  pairs at back-to-back charged tracks is observed. Unfortunately, the  $\eta$  signal itself does not reproduce this pattern as shown in Fig. 2(b). Crosses correspond to the distribution (normalized to 1) of the  $\eta$  signal in the data. The background under the  $\eta$  peak is subtracted by fitting  $M_{\gamma\gamma}$  distributions for each bin of the  $\cos(\text{charged, charged})$  independently. The histograms represent the distributions of  $\eta$ s coming from  $\tau$  decays simulated with various Monte Carlo models. The Monte Carlo signals are strongly peaked for back-to-back charged tracks, whereas the  $\eta$  signal in the data has a flat distribution. Moreover, the events containing the  $\eta$  signal in the data have a rather high sphericity, rather than a jet-jet topology (Fig. 3), and seem to be associated with higher multiplicities than expected from the Monte Carlo simulation of  $\tau$  decays to  $\eta$  (Fig. 4). After more stringent topological cuts (like those described in section 2) are added to the old event selection the  $\eta$  signal disappears completely while the detection efficiency for  $\tau$  decays to  $\eta$  decreases only by about 20 %. We conclude that the  $\eta$  signal observed in the old analysis does not stem from any of the simulated  $\tau \rightarrow \eta$  decays, which cover all relevant known possibilities. It appears, therefore, that the observed signal was due to a non- $\tau$  decay background.

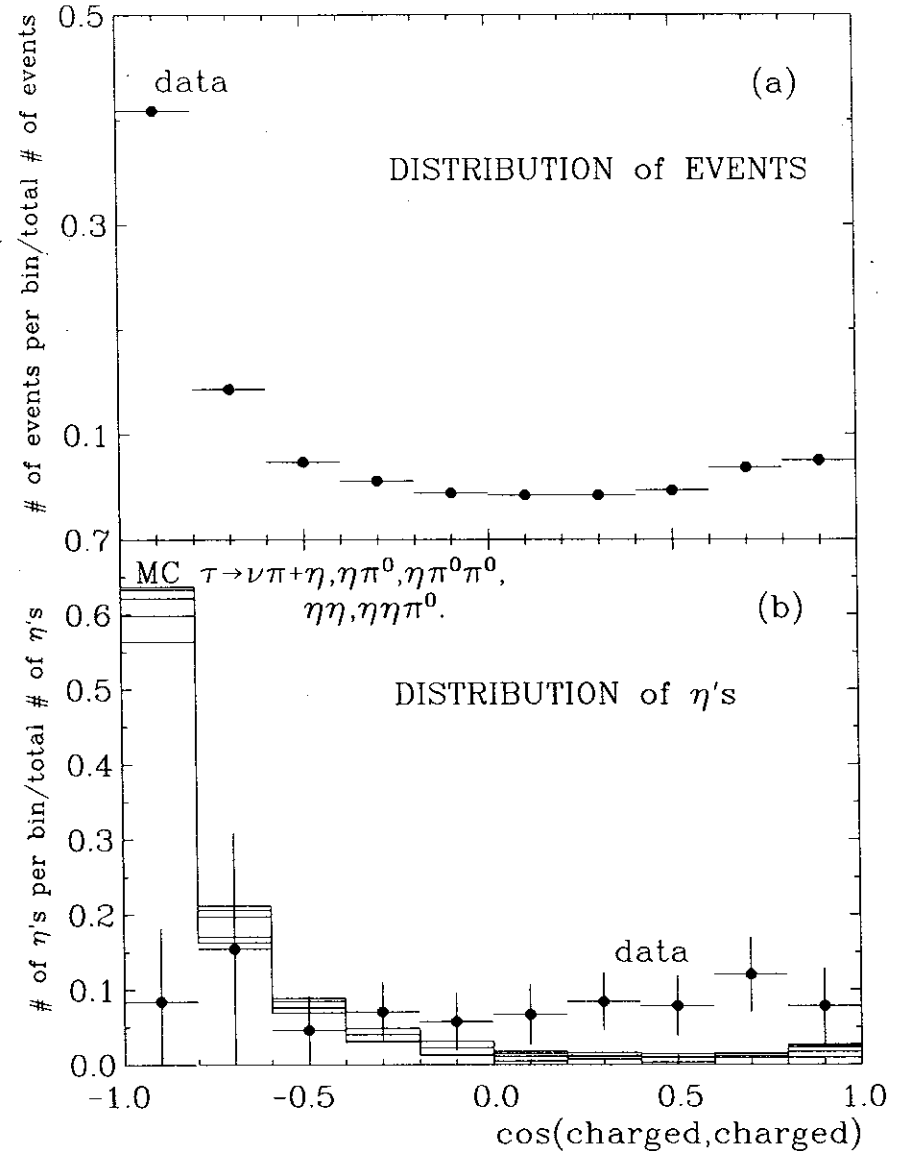


Figure 2: Distribution of the cosine of the angle between the two charged particles. All distributions are normalized to 1.

(a) Distribution for all events used in the old inclusive analysis.

(b) Distribution for events with reconstructed  $\eta$  in the old inclusive analysis (points with error bars), compared to the Monte Carlo distributions of various  $\tau$  decays to  $\eta$  (histograms).

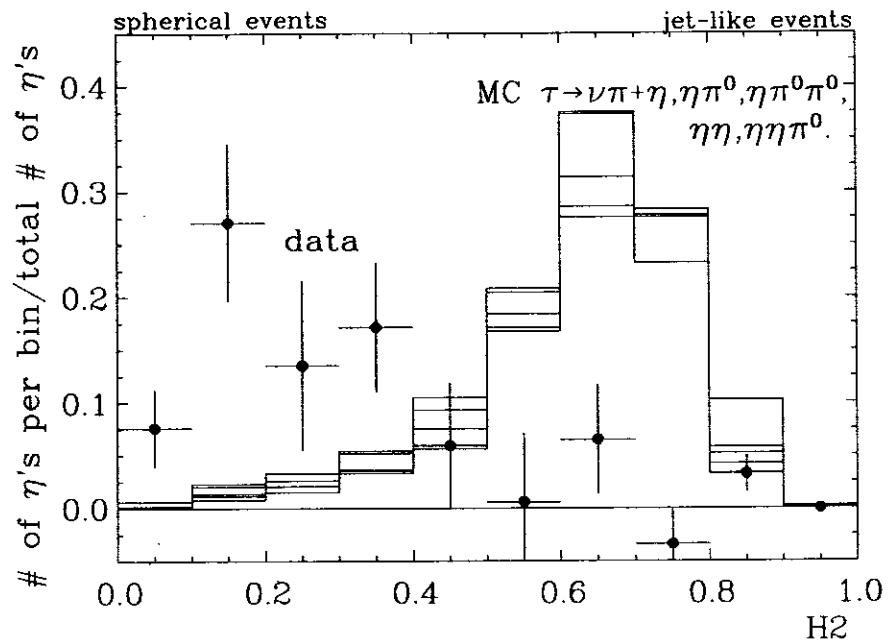


Figure 3: Distribution of the event shape parameter  $H_2$  for events with reconstructed  $\eta$  in the old inclusive analysis (points with error bars), compared to the distributions of the  $\eta$  signals in various Monte Carlo samples (histograms). The distributions are normalized to 1.

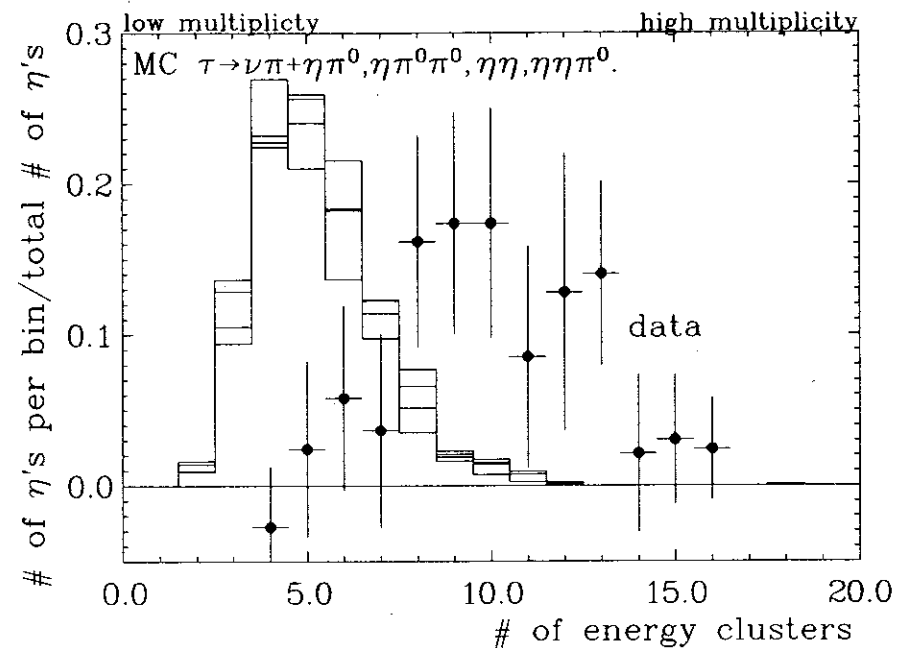


Figure 4: Visible multiplicity distribution for events with reconstructed  $\eta$  in the old inclusive analysis (points with error bars) compared to the distributions of various Monte Carlo samples (histograms). The distributions are normalized to 1.

## 4 Exclusive Analyses

In order to demonstrate our ability to correctly measure a branching ratio of  $\tau$  decaying to neutral mesons, we have performed two exclusive analyses of the final states with one or two neutral mesons. The previously well measured [4]  $\tau$  decays to the  $\rho(770)$  resonance,  $\tau^- \rightarrow \nu \rho^-$ ,  $\rho^- \rightarrow \pi^- \pi^0$ , are observed here with high statistics.  $\tau$  decays to the  $a_1(1270)$  resonance,  $\tau^- \rightarrow \nu a_1^-$ ,  $a_1^- \rightarrow (3\pi)^-$ , measured previously [4] in the three charged pion mode,  $\pi^- \pi^+ \pi^-$ , are reconstructed here for the first time in the hadronic final state,  $\pi^- \pi^0 \pi^0$ . At the same time, final states with the  $\eta$  meson are not observed.

To maintain the maximal correspondence between the inclusive and the exclusive analyses, the selection criteria used in the inclusive analysis are applied with no further retuning in the exclusive analyses. The only exception is a lower cut on photon energy ( $E_\gamma > 20$  MeV instead of  $> 50$  MeV). The cut used in the inclusive search for  $\eta$ s has to be lowered for efficient reconstruction of  $\pi^0$ s which have a lower mass. An independent Crystal Ball Collaboration analysis of  $\tau$  decays to neutral mesons dedicated to the optimal reconstruction of various exclusive final states has been presented elsewhere [15].

In the inclusive analysis, we try to reconstruct only the  $\eta$  mesons and not the other decay products, in order to be sensitive to any possible production mechanism. Therefore, the number and types of the neutral energy clusters are not constrained to a certain pattern. In contrast, in the exclusive analysis, a final state is identified by reconstruction of all the particles (except the  $\nu$ , of course). Thus, the number and type of all neutral energy clusters in the event are defined.

### 4.1 Exclusive Analysis of $\tau^- \rightarrow \nu \pi^- h^0$ , $h^0 = \pi^0$ or $\eta$ .

To study the decays  $\tau^- \rightarrow \nu \pi^- \pi^0$  and  $\tau^- \rightarrow \nu \pi^- \eta$ , events with exactly two charged and two neutral energy clusters are selected. The neutral energy clusters must be of a single photon type. The direction of the two-photon system must be within  $90^\circ$  of the charged- $\pi$  direction. The invariant mass of these two photons is plotted in Fig. 5. A prominent  $\pi^0$  peak due to  $\tau^- \rightarrow \nu \pi^- \pi^0$  events is observed. There is no enhancement seen at the  $\eta$  mass. To calculate the corresponding branching ratio (upper limit), the spectrum is fitted with the  $\pi^0$  ( $\eta$ ) line shape on a smooth polynomial background.

The fitted number of  $\tau^- \rightarrow \nu \pi^- \eta$  decays is  $2 \pm 12$  events. This corresponds to the 95% upper limit,  $\text{BR}(\tau^- \rightarrow \nu \pi^- \eta) < 0.5\%$ . A systematic error of 20% is included. The decays  $\tau^- \rightarrow \nu \pi^- \eta$  have been simulated with two different models, a phase space decay and a  $a_0(980)$  resonance production. No difference in the detection efficiency is observed. The upper limit obtained in the inclusive analysis is slightly better than the exclusive result. The selection efficiency is lower in the exclusive approach because events with spurious photons, produced by interaction of the charged hadrons in the calorimeter, are rejected.

We observe  $887 \pm 33$   $\tau^- \rightarrow \nu \pi^- \pi^0$  events, with an estimated feed-down from higher multiplicity  $\tau$  decays to  $\pi^0$ s of  $13 \pm 3$  events. This corresponds to a branching ratio of  $(23.4 \pm 0.9 \pm 3.0)\%$ , where the first error is statistical, and the second is systematic. Charged pions cannot be distinguished from charged kaons in our detector, thus the value given includes a contribution from  $\tau^- \rightarrow \nu K^- \pi^0$  decays which is expected to be  $(0.7 \pm 0.1)\%$ . The efficiency calculation assumes that all  $\tau^- \rightarrow \nu \pi^- \pi^0$  decays proceed via production of the  $\rho$  resonance, which is well supported by other experiments [16]. The branching ratio obtained (kaon con-

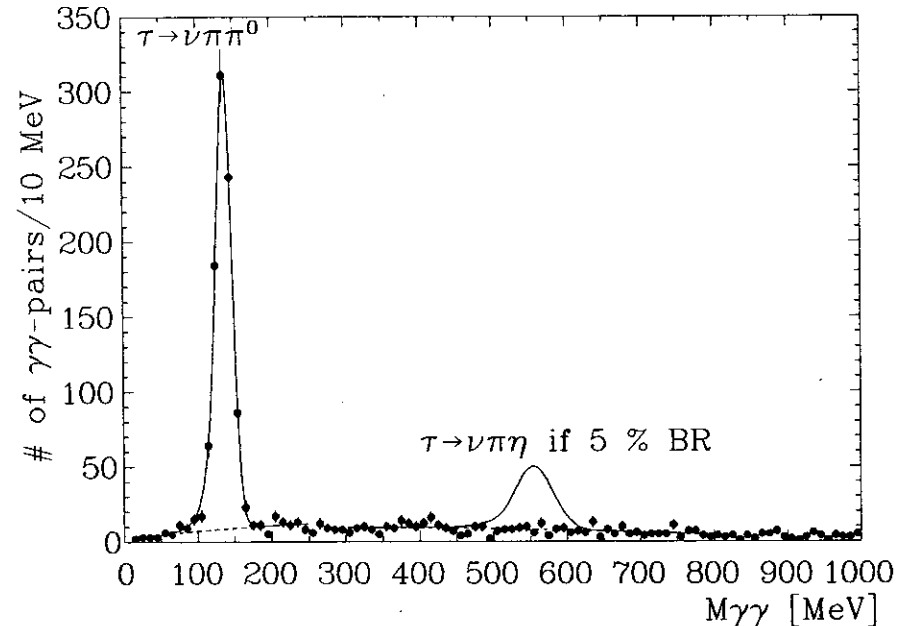


Figure 5: Two-photon invariant mass distribution in the event sample with two charged tracks and two photons. The expected size of the  $\eta$  signal from  $\tau^- \rightarrow \nu \pi^- \eta$  decays with 5% branching ratio is indicated.

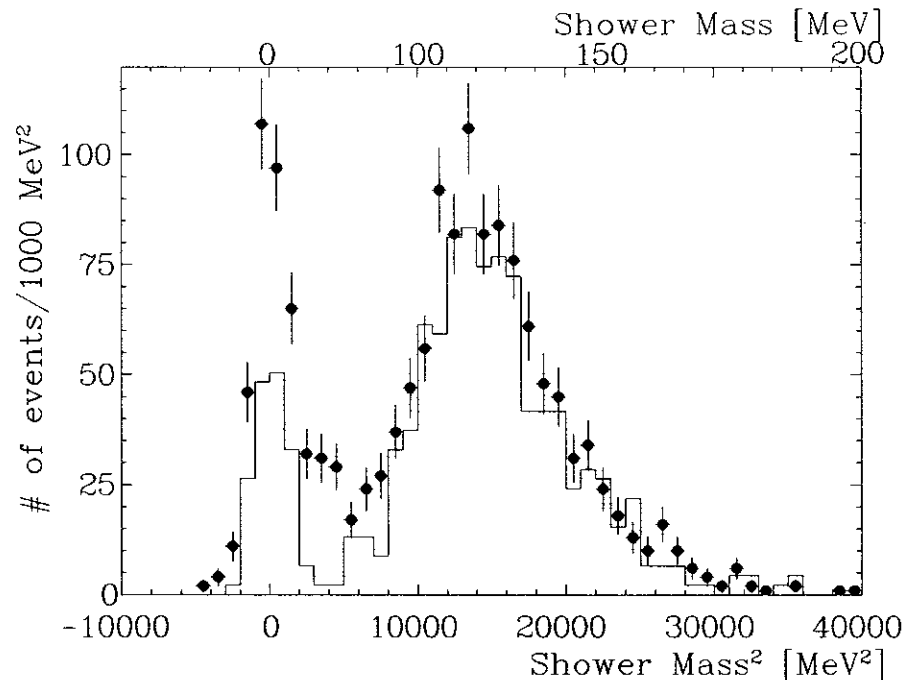


Figure 6: Shower mass squared of the neutral energy cluster in the event sample with two charged and a neutral track (points with error bars). The data are compared to the distribution for the Monte Carlo sample of  $\tau^- \rightarrow \nu \rho^-$  decays (histogram). The normalization of the Monte Carlo distribution assumes  $\text{BR}(\tau^- \rightarrow \nu \rho^-) = 22.1\%$ .

tribution subtracted),  $\text{BR}(\tau^- \rightarrow \nu \pi^- \pi^0) = (22.7 \pm 0.9 \pm 3.0)\%$ , agrees very well with the world average [4],  $\text{BR}(\tau^- \rightarrow \nu \pi^- \pi^0) = (22.1 \pm 1.1)\%$ .

The above result is obtained using two separated photons to reconstruct the  $\pi^0$ . When the  $\pi^0$  is fast enough, the two photons merge in the calorimeter and only one energy cluster is observed. An invariant mass of the overlapping showers can, nevertheless, be calculated. Here, we use a technique similar to that used in some calorimetric experiments where the mass of a jet is calculated without disentangling the individual particles in the jet. The mass of the shower is calculated from its transverse energy spread in the calorimeter. Energies and directions of the individual photons are not disentangled. Events with two charged particles and only one neutral energy cluster instead of two, as described previously, have been selected. The shower mass squared for these neutral energy clusters is plotted in Fig. 6 (points with error bars). A peak at the  $\pi^0$  mass is observed. A second peak observed at zero is due to the single photon showers. The histogram corresponds to the Monte Carlo simulation of  $\tau^- \rightarrow \nu \rho^-$  decays, where the Monte Carlo distribution has been scaled to the number of expected  $\tau^- \rightarrow \nu \rho^-$  decays in the data assuming the nominal 22.1% branching ratio. The data coincides well in shape and magnitude of the  $\pi^0$  peak with the Monte Carlo distribution, demonstrating that  $\tau^- \rightarrow \nu \pi^- \pi^0$  decays can be correctly measured using merged

$\pi^0$ s as well. The single-photon peak is larger in the data than expected from  $\tau^- \rightarrow \nu \pi^- \pi^0$  decays with one photon from the  $\pi^0$  decay missing the calorimeter. The excess comes from the  $e^+e^- \rightarrow \mu^+\mu^-\gamma$  background which is not suppressed by the cuts described in section 2. This kind of background can, however, be easily rejected by a cut on the shower mass as the  $\pi^0$  and the single-photon peaks are well resolved (see Fig. 6).

The best result on  $\text{BR}(\tau^- \rightarrow \nu \rho^-)$  can be obtained combining the data with merged and open  $\pi^0$ s from  $\rho$  decays. Such an analysis of our data, yielding the most precise value of the above branching ratio from a single experiment, is presented in ref.[15].

## 4.2 Exclusive Analysis of $\tau^- \rightarrow \nu \pi^- \pi^0 h^0$ , $h^0 = \pi^0$ or $\eta$ .

The shower mass technique, described in the previous section, proves very useful in reconstruction of the higher multiplicity channels,  $\tau^- \rightarrow \nu \pi^- \pi^0 \pi^0$  and  $\tau^- \rightarrow \nu \pi^- \pi^0 \eta$ . Although they can be detected with events with four separated photons, the detection efficiency is higher for the topology with one  $\pi^0$  open and the other one merged.

Events with exactly two charged and three neutral energy clusters are selected. The two neutral energy clusters must resemble separated photons, and the third becomes a merged- $\pi^0$  candidate. Both neutral mesons, reconstructed either from the two separated or merged photons, must have directions contained in the hemisphere along the charged- $\pi$  direction. In addition, at least one must be closer than  $40^\circ$  to the charged- $\pi$  direction. These cuts suppress a feed-down from  $\tau\tau$  pairs with both  $\tau$ s decaying to  $\rho$ s, therefore producing events with two charged tracks and two  $\pi^0$ s.

The invariant mass of the two photons,  $M_{\gamma\gamma}$ , is plotted against the shower mass squared of the third neutral energy cluster (Fig. 7). Clear clustering of  $\pi^0\pi^0$  events is observed. After a cut on the shower mass, the events are projected onto the  $M_{\gamma\gamma}$  axis (Fig. 8). A prominent  $\pi^0$  peak due to  $\tau^- \rightarrow \nu \pi^- \pi^0 \pi^0$  decays is observed on a low background. There is no signal from  $\tau^- \rightarrow \nu \pi^- \pi^0 \eta$  decays.

There is only one event at the  $\eta$  mass in the  $M_{\gamma\gamma}$  distribution (Fig. 8). It corresponds to the upper limit,  $\text{BR}(\tau^- \rightarrow \nu \pi^- \pi^0 \eta) < 3.2\%$  at 95% CL.

The fit of a  $\pi^0$  signal on a smooth background (Fig. 8) gives  $150 \pm 13$   $\pi^0\pi^0$  events. A feed-down from double  $\tau^- \rightarrow \nu \rho^-$  decays estimated by the Monte Carlo simulation is  $(4.2 \pm 2.1)\%$  of the total sample. A feed-down from the higher multiplicity  $\tau$  decays to  $\pi^0$ s, e.g.,  $\tau^- \rightarrow \nu \pi^- \pi^0 \pi^0 \pi^0$ , is below 1% of all signal events. After the background is subtracted, a branching ratio of  $(7.0 \pm 0.7 \pm 1.4)\%$  is obtained<sup>2</sup> for  $\tau^- \rightarrow \nu \pi^- \pi^0 \pi^0$  decays. Additional data with four separated photons only slightly improves the statistics of the  $\tau^- \rightarrow \nu \pi^- \pi^0 \pi^0$  events (see [15]).

To further check the analysis, we apply cuts on the energy deposition by the tagging charged prong, in an attempt to select a subsample of  $\tau^- \rightarrow \nu \pi^- \pi^0 \pi^0$  events tagged by different decay modes of the second  $\tau$  in the event, namely  $\tau^- \rightarrow \nu e^- \bar{\nu}_e$ ,  $\tau^- \rightarrow \nu \mu^- \bar{\nu}_\mu$  and  $\tau^- \rightarrow \nu \pi^-$ .

- The first subsample is obtained with cuts on the transverse energy deposition by the tagging prong designed to identify electrons.

<sup>2</sup> The preliminary number,  $\text{BR}(\tau^- \rightarrow \nu \pi^- \pi^0 \pi^0) = (6.6 \pm 0.7 \pm 1.7)\%$ , reported at the International Europhysics Conference on High Energy Physics, Uppsala, Sweden, June 25-July 1, 1987, has changed to  $(7.0 \pm 0.7 \pm 1.4)\%$  after an increase in Monte Carlo statistics used in the efficiency calculation.



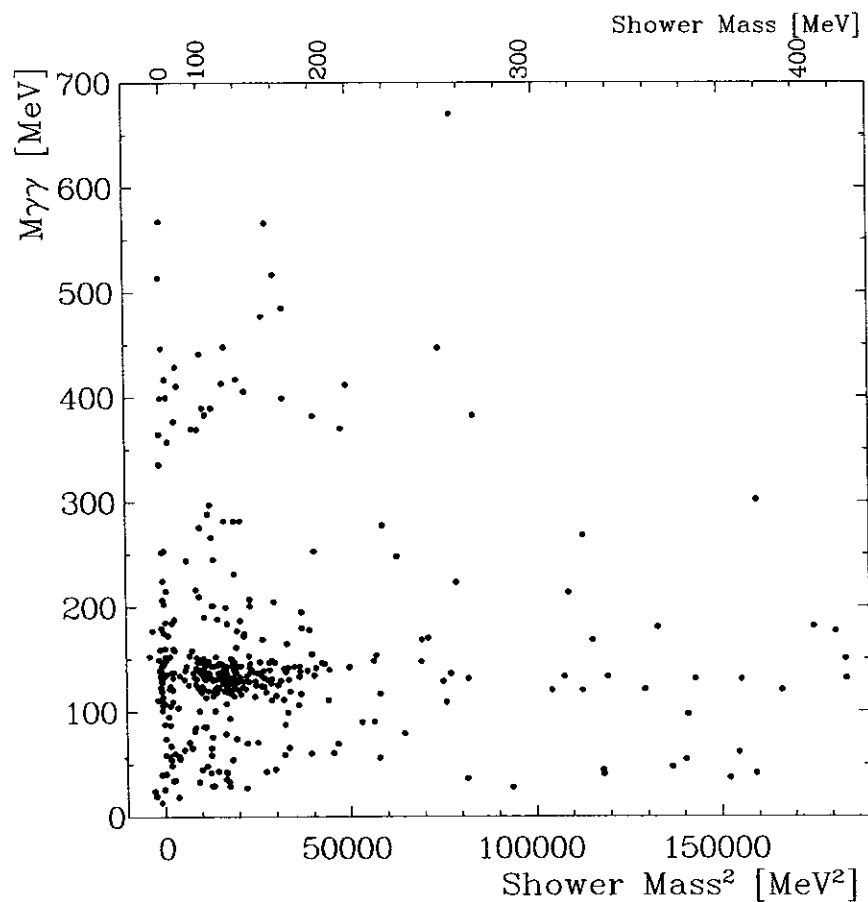


Figure 7: Two-photon invariant mass vs. shower mass squared of the neutral energy clusters in the event sample with two charged and three neutral tracks. Events clustering around the  $\pi^0$  mass on the both axes come from  $\tau^- \rightarrow \nu\pi^-\pi^0\pi^0$  decays.

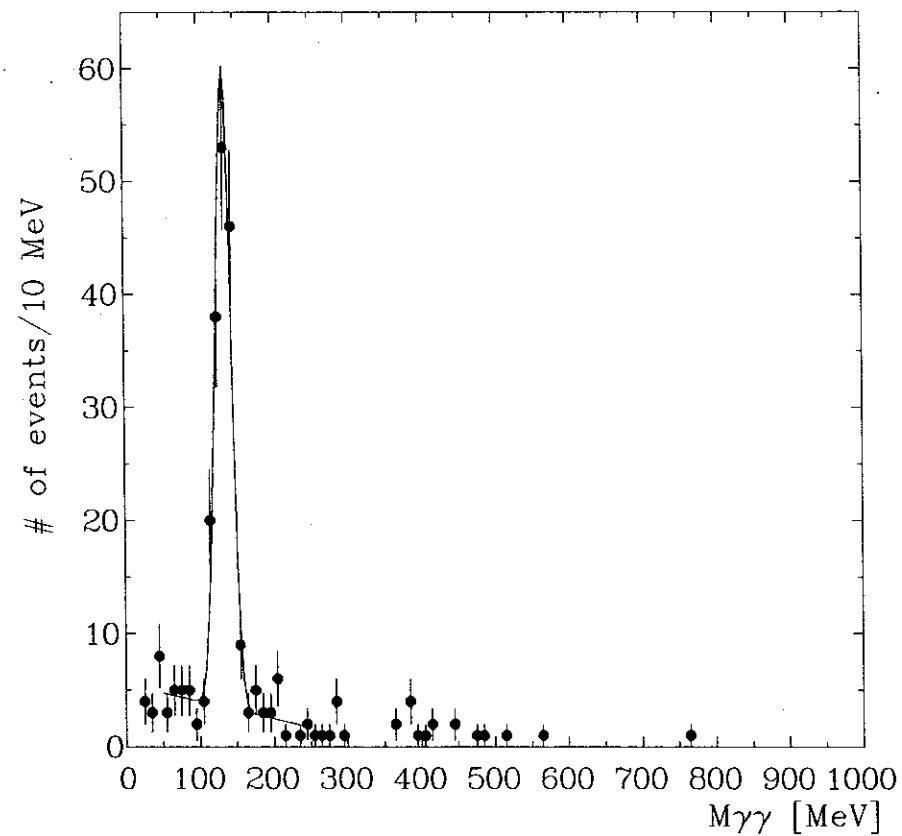


Figure 8: Invariant mass of the two photons in the event sample with two charged and three neutral tracks after the merged  $\pi^0$  has been identified by the shower mass technique. The  $\pi^0$  peak corresponds to  $\tau^- \rightarrow \nu\pi^-\pi^0\pi^0$  decays.

- The second subsample corresponds to the tagging prong which leaves a minimum ionizing pattern in the calorimeter, characteristic of muons and charged pions which do not interact in the detector.
- All tagging prongs which do not pass either the electron or the minimum ionizing cuts are classified as the third category. Electrons failing stringent identification criteria and charged pions interacting in the NaI crystals give the main contributions here.

There is a good  $\pi^-\pi^0\pi^0$  signal in all three subsamples (Fig. 9). The results for  $\text{BR}(\tau^- \rightarrow \nu\pi^-\pi^0\pi^0)$  obtained from these three statistically independent subsamples are listed in Table 1. They agree well, showing that there is no large systematic error in the background subtraction and in the determination of the tagging efficiencies.

Table 1:  $\text{BR}(\tau^- \rightarrow \nu\pi^-\pi^0\pi^0)$  obtained with different tags. The errors are statistical only, where fluctuations of the experimental data and of the Monte Carlo data used in the efficiency calculation have been added in quadrature. Estimated contributions from the main  $\tau$  decay modes are given in percent of all tags. Remaining contributions come from the other  $\tau$  decays.

tag	contribution from ...			$\text{BR}(\tau^- \rightarrow \nu\pi^-\pi^0\pi^0)$ in %
	$\tau^- \rightarrow \nu e^- \bar{\nu}_e$	$\tau^- \rightarrow \nu \mu^- \bar{\nu}_\mu$	$\tau^- \rightarrow \nu \pi^-$	
electron	88%	2%	2%	$6.8 \pm 1.5$
minimum ionizing	0%	76%	21%	$6.3 \pm 1.3$
other	50%	10%	32%	$7.7 \pm 2.1$

Since the momentum of the charged- $\pi$  is not measured, the invariant mass of the  $3\pi$  system cannot be reconstructed. Therefore, we cannot look directly for the  $a_1(1270)$  resonance structure, which is observed in the three-charged- $\pi$  decay mode of  $\tau$  [17]. However, we calculate a pseudo-mass of the hadronic system ignoring a difference between the visible and the true charged pion energy. The distribution of the pseudo-mass in the data can be compared with Monte Carlo simulations of  $\tau^- \rightarrow \nu\pi^-\pi^0\pi^0$  decays proceeding via  $a_1(1270)$  resonance or phase space production. The comparison is shown in Fig. 10. The data are clearly inconsistent with phase space decay and agree very well with  $a_1(1270)$  resonance production.

This analysis yields the first reconstruction of  $\tau^- \rightarrow \nu\pi^-\pi^0\pi^0$  events, where the both  $\pi^0$ s are identified. The feed-down from other  $\tau$  decays is very small in contrast with earlier attempts to measure  $\text{BR}(\tau^- \rightarrow \nu\pi^-\pi^0\pi^0)$  indirectly, i.e., without  $\pi^0$  identification. Results for the  $\text{BR}(\tau^- \rightarrow \nu\pi^-\pi^0\pi^0)$  from indirect measurements [5,18,19] are inconsistent among themselves. Our direct measurement provides a value in between these indirect results.

The obtained branching ratio for  $\tau^- \rightarrow \nu\pi^-\pi^0\pi^0$  decays,  $(7.0 \pm 0.7 \pm 1.4)\%$ , agrees very well with the measured branching ratio for  $\tau^- \rightarrow \nu\pi^-\pi^+\pi^-$ ,  $(6.6 \pm 0.6)\%$  [4]. In fact, this is expected [3] from isospin symmetry and  $a_1(1270)$  dominance of the  $3\pi$  production established by the 3-prong data [17].

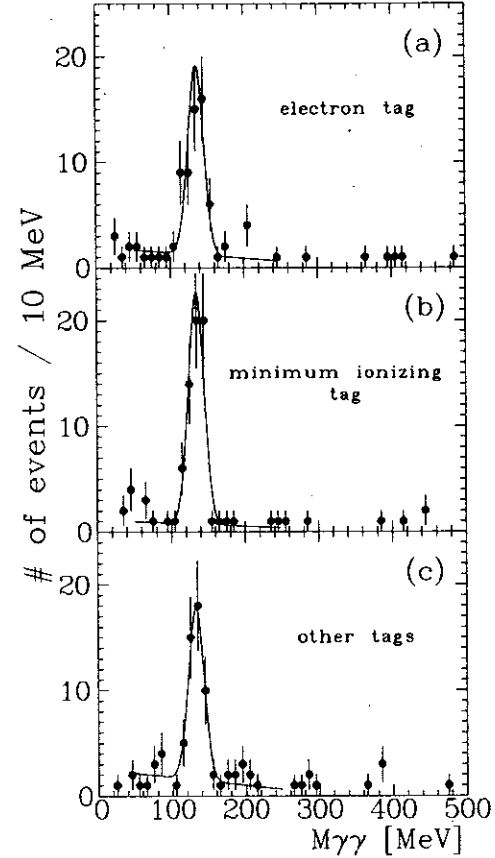


Figure 9: Invariant mass distributions of the two photons in the event samples with two charged and three neutral tracks after the merged  $\pi^0$  has been identified by the shower mass technique. The  $\pi^0$  peaks correspond to the  $\tau^- \rightarrow \nu\pi^-\pi^0\pi^0$  signals.

(a) Events with the tagging prong passing the electron identification cuts.

(b) Events with the tagging prong passing the minimum ionizing cut.

(c) Events with the tagging prong failing the electron and minimum ionizing cuts.

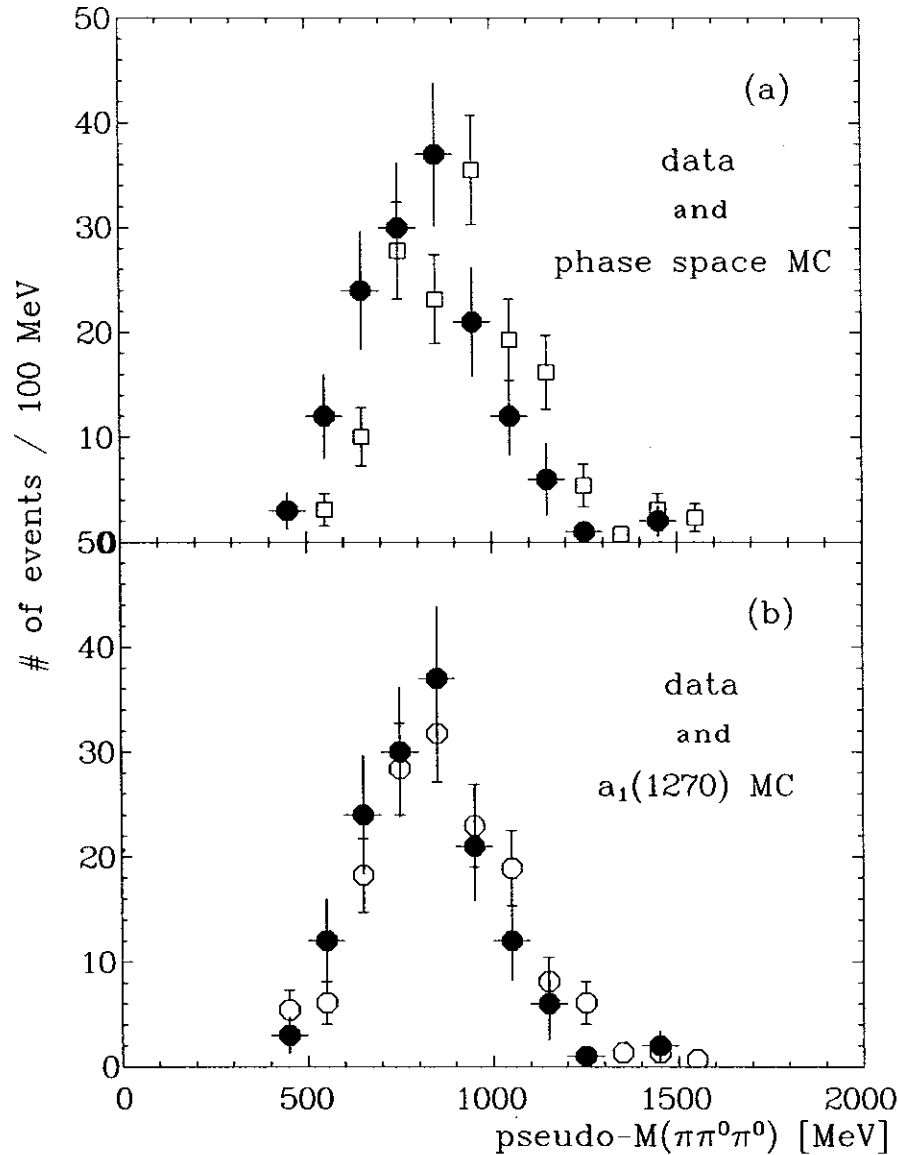


Figure 10: The pseudo-invariant-mass of the  $\pi^-\pi^0\pi^0$  system in the reconstructed  $\tau^- \rightarrow \nu\pi^-\pi^0\pi^0$  events (full points).

(a) Compared to the distribution of the Monte Carlo events with the invariant three-pion-mass generated according to the phase space (open points).

(b) Compared to the distribution of the Monte Carlo events with the invariant three-pion-mass generated according to the  $a_1(1270)$  resonance excitation (open points).

The Monte Carlo distributions are scaled to the data assuming  $\text{BR}(\tau^- \rightarrow \nu\pi^-\pi^0\pi^0) = 7.0\%$ .

## 5 Summary and Conclusions

We have searched for  $\eta$  production in  $\tau$  decays. Contrary to earlier reports [10], there is no evidence for such production in the inclusive analysis of 1-prong  $\tau$  decays. This is confirmed for the lowest multiplicity decay modes,  $\tau^- \rightarrow \nu\pi^-\eta$  and  $\tau^- \rightarrow \nu\pi^-\pi^0\eta$ , in the exclusive analyses, where we also demonstrate our ability to correctly measure branching ratios of the decays,  $\tau^- \rightarrow \nu\pi^-\pi^0$  and  $\tau^- \rightarrow \nu\pi^-\pi^0\pi^0$ .

Our limit on the second class current decay,  $\text{BR}(\tau^- \rightarrow \nu\pi^-\eta) < 0.3\%$  (95% CL), is more than an order of magnitude smaller than the branching ratio previously claimed.

We also do not find any other  $\tau$  to  $\eta$  decays. The upper limits are set, which imply that any  $\eta$  production in  $\tau$  decays will not explain the unaccounted topological 1-prong branching ratio of the  $\tau$  lepton. This has been predicted earlier on theoretical grounds [8]. In theory, the decay,  $\tau^- \rightarrow \nu\pi^-\pi^0\eta$ , is expected to have the highest branching ratio among all  $\tau$  decays to  $\eta$  [21]. We obtain the limit on this decay,  $< 0.9\%$  (95% CL), which is well above the predicted branching ratio, 0.2–0.3% [8,21].

In the exclusive analysis, we measure the  $\tau^- \rightarrow \nu\pi^-\pi^0$ . A branching ratio agrees with the earlier measurements. The first reconstruction of  $\tau^- \rightarrow \nu\pi^-\pi^0\pi^0$  events is presented. The corresponding branching ratio agrees very well with the expectation from  $\tau^- \rightarrow \nu\pi^-\pi^+\pi^-$  measurements, isospin symmetry, and  $a_1(1270)$  dominance of the  $3\pi$  production. Therefore, the anomaly in 1-prong  $\tau$  decays remains an unsolved puzzle.

## References

- [1] The Crystal Ball collaboration :  
D. Antreasyan, D. Besset, Ch. Bieler, J.K. Bienlein, E.D. Bloom, I. Brock, R. Cabenda, A. Cartacci, M. Cavalli-Sforza, R. Clare, G. Conforto, S. Cooper, R. Cowan, D. Coyne, A. Engler, K.H. Fairfield, G. Folger, A. Fridman, J. Gaiser, D. Gelpman, G. Godfrey, F.H. Heimlich, J. Irion, Z. Jakubowski, S. Keh, H.H. Kilian, I. Kirkbride, T. Kloiber, W. Koch, A.C. König, K. Königsmann, R.W. Kraemer, G. Landi, R. Lee, S. Lefler, R. Lekebusch, P. Lezoch, A.M. Litke, W. Lockman, S. Lowe, B. Lurz, D. Marlow, W. Maschmann, T. Matsui, P. McBride, F. Messing, W.J. Metzger, B. Monteleoni, B. Muryn, R. Nernst, C. Newman-Holmes, B. Niczyporuk, G. Nowak, C. Peck, P.G. Pelfer, B. Pollock, F.C. Porter, D. Prindle, P. Ratoff, B. Renger, C. Rippich, M. Scheer, P. Schmitt, J. Schotanus, A. Schwarz, D. Sievers, T. Skwarnicki, K. Strauch, U. Strohmusch, J. Tompkins, H.J. Trost, R.T. Van de Walle, H. Vogel, U. Volland, K. Wachs, K. Wacker, W. Walk, H. Wegener, D. Williams, P. Zschorsch,  
*California Institute of Technology, Pasadena, CA 91125,*  
*Carnegie-Mellon University, Pittsburgh, PA 15213,*  
*Cracow Institute of Nuclear Physics, Cracow, Poland,*  
*Deutsches Elektronen Synchrotron DESY, Hamburg, Germany,*  
*Universität Erlangen-Nürnberg, Erlangen, Germany,*  
*INFN and University of Firenze, Italy,*  
*Universität Hamburg, I. Institut für Experimentalphysik, Hamburg, Germany,*  
*Harvard University, Cambridge, MA 02138,*  
*University of Nijmegen and NIKHEF-Nijmegen, The Netherlands,*  
*Princeton University, Princeton, NJ 08544,*  
*Department of Physics, HELP, and Stanford Linear Accelerator Center,*  
*Stanford University, Stanford, CA 94305,*  
*Universität Würzburg, Würzburg, Germany.*
- [2] P. R. Burchat, Proceedings of the XXIII International Conference on High Energy Physics, Berkeley, California, July 16-23, 1986, ed. S.C. Loken, p. 756.
- [3] F.J. Gilman, S.H. Rhie, Phys. Rev. **D31**, 1066 (1985).
- [4] For a recent review of  $\tau$  properties see:  
B.C. Barish, R. Stroynowski. CALT-68-1425, April 1987, submitted to Phys. Rep.
- [5] H. Aihara *et al.* (TPC), Phys. Rev. Lett. **57**, 1836 (1986).
- [6] P.R. Burchat *et al.* (Mark-II), Phys. Rev. **D35**, 27 (1987).
- [7] Particle Data Group, Phys. Lett. **170B** (1986).
- [8] F.J. Gilman, SLAC-PUB-4265, March 1987, submitted to Phys. Rev. Rapid Communications.
- [9] M. Derrick *et al.* (HRS), Phys. Lett. **B189**, 260 (1987).
- [10] M. G. Gilchriese, Proceedings of the XXIII International Conference on High Energy Physics, Berkeley, California, July 16-23, 1986, ed. S.C. Loken, p. 140.
- [11] M. Oreglia *et al.*, Phys. Rev. **25**, 2259 (1982), M. Oreglia, Ph.D. Thesis, Stanford University 1980, SLAC Report 236,  
Bloom E., C. Peck, Ann. Rev. Nucl. Part. Sci. **33**: 149 (1983).
- [12] F.A. Berends, R. Kleiss, Nucl. Phys. **B177**, 239 (1981).
- [13] G. C. Fox, S. Wolfram, Phys. Rev. Lett. **41**, 1581 (1978).  
H2 is defined as,  

$$H2 \equiv \frac{\sum_i \sum_j E_i E_j (3 \cos^2 \alpha_{ij} - 1)}{2(\sum_k E_k)^2}$$

where  $E_i$  is an energy deposition in the NaI(Tl) crystal,  
and  $\alpha_{ij}$  is an angle between the two crystals.

Spherical events populate low H2 values, whereas jet like events exhibit large H2 ( $0 \leq H2 \leq 1$ ).
- [14]  $E_T$  is defined as :  

$$E_T \equiv \sum_i E_i \sin \theta_i$$

where  $\theta_i$  is a polar angle of the NaI(Tl) crystal with respect to the beam direction.
- [15] S. T. Lowe (Crystal Ball), Proceedings of the International Symposium on Production and Decay of Heavy Flavors, Stanford, California, September 1-5, 1987, SLAC-PUB-4449 (1987).
- [16] J.M. Yelton *et al.* (Mark-II), Phys. Rev. Lett. **56**, 812 (1986),  
H.J. Behrend *et al.* (CELLO), Z. Phys. **23**, 103 (1984).
- [17] H. Albrecht *et al.* (ARGUS), Z. Phys. **C33**, 7 (1986),  
H. Albrecht *et al.*, DESY 86-142.
- [18] K.K. Gan *et al.* (Mark-II), Phys. Rev. Lett. **59**, 411 (1987).
- [19] H.R. Band *et al.* (MAC), SLAC-PUB-4333 (1987) submitted to Phys. Lett.
- [20] For a review of new experimental data on  $\tau$  decays to  $\pi^0$ s and  $\eta$ s see:  
T. Skwarnicki, Proceedings of the International Europhysics Conference on High Energy Physics, Uppsala, Sweden, June 25-July 1, 1987.
- [21] A. Pich, CERN-TH.4717/87, May 1987.